Role of the Hexapeptide Disulfide Loop in the γ-Carboxyglutamic Acid Domain of Protein C in Ca^{2+}-Mediated Structural and Functional Properties†

Qiuyun Dai, Mary Prorok, and Francis J. Castellino*

Department of Chemistry and Biochemistry and the W. M. Keck Center for Transgene Research, University of Notre Dame, Notre Dame, Indiana 46556

Received May 25, 2005; Revised Manuscript Received July 21, 2005

ABSTRACT: The anticoagulant and immunomodulatory effects of protein C (PC) rely on the presence of the N-terminal γ-carboxyglutamic acid (Gla) domain. This domain is strongly conserved among vitamin K-dependent blood proteins and, in addition to a high relative content of Gla, contains a hexapeptide disulfide loop between Cys residues 17 and 22. In the present study, the contribution of the hexapeptide loop toward Gla domain structure and function was evaluated using wild-type and Cys17/Cys22-alkylated synthetic peptide analogues of the 47-residue Gla domain/helical stack of PC. Circular dichroism and intrinsic fluorescence measurements revealed significant differences in the metal ion-dependent conformations of the two peptides. Disruption of the disulfide loop slightly altered the capacity of the peptide to interact with acidic phospholipid (PL) vesicles. The affinity of the alkylated peptide for soluble endothelial protein C receptor (EPCR), as demonstrated by surface plasmon resonance studies, was increased compared with the wild-type species, although total binding was compromised. These results suggest that the disulfide loop of PC contributes to the overall Ca^{2+}-dependent conformation but is not strictly required for PL membrane binding or EPCR recognition.

Protein C (PC) is a member of the class of vitamin K dependent plasma proteins and shares extensive amino acid sequence homology and domain organization with other zymogens of this type, including factors (F) VII, IX, and X. PC is a major regulatory component of the hemostatic system, functioning in both anticoagulant and profibrinolytic capacities. The conversion of PC to activated protein C (APC)[1] is catalyzed optimally by thrombin in complex with thrombomodulin on the membrane surface. The APC thus formed inhibits further generation of thrombin by proteolysis of cofactors FVa and FVIIIa (*1*). In addition, APC enhances clot lysis through the inactivation of plasminogen activator inhibitor type 1 (PAI-1) and the downregulation of thrombin-activated fibrinolysis inhibitor (TAFI) (*2*, *3*). More recently, antiinflammatory and antiapoptotic roles for PC have been identified (*4*, *5*). These immunomodulatory effects are regulated through the interaction of PC with its receptor target, the endothelial protein C receptor (EPCR) (*6*). This diverse array of physiological PC activities is unified by a common requirement for the conformational and/or sequence integrity of the N-terminal γ-carboxyglutamic acid (Gla) domain and the immediately adjacent helical stack region. The Ca^{2+}-induced conformation of the Gla domain (GD)−helical stack (HS) module is necessary for the interaction of PC with the phospholipid (PL) membrane, on which assembly of activation/inactivation complexes occurs (*7*, *8*). Similar membrane anchoring events are crucial to the activities of FVII, FIX, and FX and support a general role for GDs in PL binding (reviewed in ref *9*). This model has been further reinforced through PL binding studies that reveal GD interchangeability among several vitamin K-dependent protein chimeras (*10*−*12*). In contrast, the binding of PC to EPCR cannot be supplanted by GDs of other proteins, indicating that specific side chains in the GD and/or local motifs are involved in PC recognition by EPCR (*13*). A structural element present in PC, and conserved throughout the vitamin K-dependent class of blood proteins, is a hexapeptide loop maintained by a disulfide bond between Cys residues 17 and 22. This loop contains two Gla residues at sequence positions 19 and 20, only one of which (Gla20) is important for the anticoagulant and PL-binding properties of PC (*14*, *15*). A previous investigation, in which the contribution of the C17−C22 disulfide bond to the anticoagulant properties of the GD-PC was examined through site-specific mutagenesis (C22S), concluded that the Cys linkage is necessary for the anticoagulant activity of PC (*16*). However, since fully carboxylated C22S-PC represented only a small subpopulation of expressed protein, a more complete assessment of the structural and PL-binding effects engendered by elimination of the disulfide bond was not practicable. After this mutagenesis study, the EPCR and its role in enhancing PC activation were identified (*17*). A recent crystal structure of the GD-PC complexed with soluble EPCR ascribes the bulk of the binding energy to contacts between L82 and Y154 of EPCR and ω-loop residues F4 and L8 of

† This work was supported by National Institutes of Health Grant HL-19982 to F.J.C.

* Corresponding author. Telephone: (574) 631-9152. Telefax: (574) 631-8017. E-mail: fcastell@nd.edu.

[1] Abbreviations: APC, activated protein C; EPCR, endothelial cell protein C/APC receptor; sEPCR, soluble recombinant EPCR; Gla, γ-carboxyglutamic acid; PL, phospholipid; CD, circular dichroism; dansyl, 5-(dimethylamino)naphthalene-1-sulfonyl; DOPC, 1,2-dioleoyl-*sn*-glycero-3-phosphocholine; DOPS, 1,2-dioleoyl-*sn*-glycero-3-phospho-L-serine; Hepes, *N*-(2-hydroxyethyl)piperazine-*N*′-2-ethanesulfonic acid; HBS, Hepes-buffered saline; PE, phosphatidylethanolamine; tBu, *tert*-butyl; TFA, trifluoroacetic acid.

10.1021/bi050974+ CCC: $30.25
Published on Web 08/25/2005

PC (*18*). The hexapeptide loop of PC resides opposite to the EPCR-PC Gla domain interface, militating against a significant intermolecular role. However, this does not rule out the possibility that the presence of the disulfide bond may be coupled to the orientation and/or mobility of ω-loop residues. Additionally, the reliance of PC anticoagulant properties upon the disulfide moiety suggests a possible linkage of this cyclic motif with optimal PL adhesion. The present study employs synthetic peptide analogues of the GD-PC to probe the relationship of the hexapeptide loop to Ca^{2+}-induced conformational effects, PL binding, and EPCR affinity.

MATERIALS AND METHODS

Peptide Synthesis, Purification, and Characterization. The GD-HS peptide amide, ANSFL$^{5}\gamma\gamma$LRH^{10}SSLγR$^{15}\gamma$CI$\gamma\gamma^{20}$-ICDF$\gamma^{25}\gamma$AKγI^{30}FQNVD^{35}DTLAF^{40}WSKHV^{45}DG-NH_2, representing the sequence counterpart to the 47 N-terminal amino acid residues (PC[1−47]), and the corresponding C17/C22 *tert*-butyl (tBu) derivatized analogue (PC[1−47-di-tBu]) were obtained from a single synthesis using a PE Applied Biosystems model 433A peptide synthesizer (Foster City, CA). Solid-phase chemistry was carried out on a 0.1 mmol scale using PAL resin (Perseptive Biosystems, Framingham, MA). N^{α}-Fmoc-(γ,γ'-di-*O*-tBu)-L-Gla was chemically synthesized as described previously (*19*). All other N^{α}-Fmoc-derivatized L-amino acids used in the synthesis were purchased from Sigma (St. Louis, MO) or Novabiochem (San Diego, CA). The following side-chain protecting groups were employed: Arg(N^{G}-2,2,4,6,7-pentamethyldihydrobenzofuran-5-sulfonyl), Asn(N^{γ}-trityl), Asp(*O*-tBu), Cys(tBu), Gln(N^{δ}-trityl), Lys(N^{ϵ}-*tert*-butyloxycarbonyl), Ser(tBu), Thr(tBu), and Trp(*N*-*tert*-butyloxycarbonyl). Each residue was double coupled at 10-fold molar excess using the manufacturer's protocols for FastMoc chemistry with the exception of derivatized Gla, which was introduced at 5-fold molar excess and allowed to couple for 90 min. The peptide was cleaved from the resin, and protecting groups were removed (excepting the tBu moiety on Cys residues 17 and 22) by treatment with 88% TFA containing 5% H_2O (v/v), 5% dithiothreitol (w/v), and 2% triisopropylsilane (v/v). After ether precipitation of the crude alkylated peptide, approximately half of the remaining material was dissolved in cold TFA. The tBu-Cys residues were deprotected by treatment with a 20-fold molar excess of $Hg(OAc)_2$. The mixture was stirred for 5 h at 4 °C. TFA was removed in vacuo. The crude peptide was dissolved in 100 mM 2-mercaptoethanol (5 mL) and allowed to stand overnight. The suspension was centrifuged, and the supernate was chromatographed on a 1.5 × 90 cm bed of Sephadex G-15 equilibrated in 0.1% NH_4OH. Fractions corresponding to peptide were pooled and lyophilized. Formation of the internal disulfide bond was accomplished by stirring a dilute peptide solution (0.2 mg/mL) in 20 mM Tris-HCl/100 mM NaCl, pH 7.8, at 4 °C for 48 h. Progress and completion of the oxidation reaction was monitored by titers with Ellman's reagent. Purification of the peptide was performed on a Bio-Rad Bio-Scale DEAE 20 anion-exchange column (Hercules, CA) equilibrated with 10 mM $NaBO_3$, pH 7.80, and eluted with a linear gradient of NaCl. Fractions containing the target peptide were combined, lyophilized, and desalted on Sephadex G-15. Purified PC[1−47-di-tBu] was obtained by subjecting the remaining portion of the initial ether precipitate to Sephadex G-15 chromatography, DEAE anion-exchange chromatography, and a final desalting step on Sephadex G-15. During all phases of purification, target peptides were characterized by analytical reverse-phase HPLC and DE-MALDI-TOF spectrometry as detailed earlier (*20*). The MALDI mass spectra were obtained in the negative ionization mode to attain fully decarboxylated species in the laser field [as opposed to the multiple, differentially decarboxylated peaks associated with the positive ion mode (*20*)]. The molecular masses obtained were 5530.1 for de-γ-carboxyl-PC[1−47] (calculated M − H = 5527.1) and 5640.7 for de-γ-carboxyl-PC[1−47-di-tBu] (calculated M − H = 5641.1).

Circular Dichroism. CD spectra were collected at 25 °C on an AVIV Model 202SF spectrometer in a 1 cm path length cell. Peptides were dissolved in 20 mM Tris-HCl/100 mM NaCl, pH 7.8, at a concentration of 50 μM. The helical content of peptides at various $CaCl_2$ or $MgCl_2$ concentrations was determined from the mean residue ellipticities at 222 nm using the empirical relationship, $\text{fraction}_{\text{helix}} = (-[\Theta]_{222} - 2340)/30300$ (*21*).

Metal-Induced Quenching of Intrinsic Peptide Fluorescence. Fluorescence measurements were conducted on a QuantaMaster steady-state spectrofluorometer (Photon Technology International, Inc., Lawrenceville, NJ) using slit widths of 2 nm (excitation) and 4 nm (emission). All measurements were performed at 25 °C in a 1 cm path length quartz cell. The excitation and emission wavelengths were 280 and 340 nm, respectively. The Gla-containing peptides were dissolved in 20 mM Tris-HCl/100 mM NaCl, pH 7.8, at a concentration of 2 μM and titrated with stock solutions of $CaCl_2$ or $MgCl_2$ prepared in the same buffer. The background fluorescence spectra were recorded and subtracted from the peptide-containing sample. Fluorescence intensities were corrected for dilution.

Interaction of Gla-Containing Peptides with Phospholipid (PL) Vesicles. Fluorescence energy transfer experiments (*22*) were employed to quantitate the binding of the wild-type and alkylated PC[1−47] peptides to acidic PL vesicles containing dansyl-PE. Interaction of the peptide with the PL bilayer permits energy transfer from W41 of the PC analogues to the dansyl-PE, leading to an increase in fluorescence at the dansyl group emission wavelength maximum of 520 nm. Dansyl-PE was purchased from Avanti Polar Lipids, Inc. (Alabaster, AL). Small unilamellar PL vesicles (DOPS:DOPC:dansyl-PE, 40:50:10 w/w/w) were prepared in 20 mM Tris-HCl/100 mM NaCl, pH 7.4, as described previously (*23*) and were used within 48 h of preparation. All measurements were performed at 25 °C in 1 cm path length semimicro quartz cuvettes containing 16 μg of PL in a total volume of 1 mL. Changes in fluorescence intensity were monitored as a function of increasing Ca^{2+} concentration in the presence of 3 μM peptide or as a function of increasing peptide concentration at 2 mM Ca^{2+}.

Peptide Binding to Human Soluble Endothelial PC Receptor (sEPCR). Surface plasmon resonance (SPR) analysis of Ca^{2+}-dependent peptide-receptor binding was performed on a Biacore 3000 instrument (Biacore Inc., Piscataway, NJ). The recombinant sEPCR employed consisted of the extracellular domain of human EPCR and a 12-residue HPC4 antibody epitope tag at the carboxyl terminus (*24*). sEPCR was immobilized on a CM5 sensor chip according to the

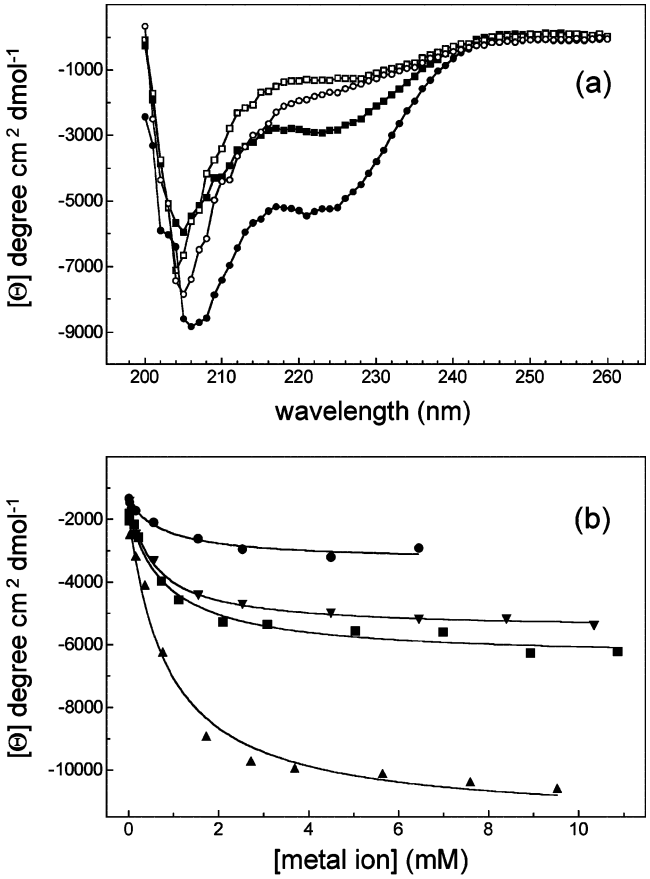

FIGURE 1: CD analysis of the effect of Ca^{2+} and Mg^{2+} on the secondary structure of PC[1−47] and PC[1−47-di-tBu]. (a) CD spectra of PC[1−47] and PC[1−47-di-tBu] in the presence and absence of 10 mM $CaCl_2$: (○) PC[1−47]; (●) PC[1−47] + Ca^{2+}; (□) PC[1−47-di-tBu]; (■) PC[1−47-di-tBu] + Ca^{2+}. (b) Effect of increasing $CaCl_2$ or $MgCl_2$ concentration on the molar ellipticity, monitored at 222 nm, of PC[1−47] and PC[1−47-di-tBu]: (■) PC-[1−47] + Ca^{2+}; (▲) PC[1−47] + Mg^{2+}; (●) PC[1−47-di-tBu] + Ca^{2+}; (▼) PC[1−47-di-tBu] + Mg^{2+}.

manufacturer's protocol for surface thiol coupling. The carboxymethylated dextran surface was activated by the injection of 45 μL of a solution containing 0.2 M 1-ethyl-3-(3-dimethylaminopropyl)carbodiimide and 0.05 M *N*-hydroxysuccinimide and modified by injection of 40 μL of 80 mM 2-(2-pyridinyldithio)ethanamine in 0.1 M borate buffer, pH 8.5. Following the activation step, a solution of sEPCR (150 μg/mL) in 10 mM sodium acetate, pH 4.0, was injected over the designated flow cells until the desired amount of immobilized protein yielded RU values of ca. 10000. Residual thiol-reactive groups on the sensor surface were quenched with a solution of 50 mM cysteine/1 M NaCl. The reference cell was treated identically to the sample cells, excepting the exclusion of sEPCR from the coupling buffer. Real-time kinetic assays were carried out at 25 °C at a flow rate of 5 μL/min. The 47-mers were dissolved in a running buffer consisting of 10 mM Hepes/100 mM NaCl/5 mM $CaCl_2$, pH 7.4. The steady-state affinities of the Gla-containing peptides for the immobilized sEPCR were determined from plots of the association phase plateau RU values versus 47-mer concentration.

RESULTS

Effect of the Hexapeptide Disulfide Loop on the Metal Ion-Dependent Conformation of the PC[1−47] Peptides. In the absence of divalent metal ions, both PC[1−47] and PC[1−47-di-tBu] display CD spectra consistent with minimal secondary structure (Figure 1a). In the presence of saturating Ca^{2+} (10 mM), the wild-type peptide adopts the spectral characteristics of an α-helix, as evidenced by the appearance of a shoulder at 222 nm. Likewise, the presence of Ca^{2+} promotes a slight increase in helicity of the alkylated 47-mer, but not to the extent observed with PC[1−47]. On the basis of the molar ellipticity values at 222 nm, PC[1−47] adopts 10% helical content in the presence of Ca^{2+}, while the di-*tert*-butylated analogue manifests 2% helicity. The addition of Mg^{2+} induces more overall helicity in the peptides than does Ca^{2+}, but the reduced responsiveness of the alkylated versus wild-type peptide, with respect to Mg^{2+}-mediated conformational change, parallels that observed with Ca^{2+} (Figure 1b). At saturating concentrations of Mg^{2+}, PC-[1−47] and PC[1−47-di-tBu] display 27% and 10% helix content, respectively. Analysis of the CD-monitored titration curves in Figure 1b reveals that, while important in maintaining secondary structure, the hexapeptide loop does not significantly influence the metal ion concentration required for the CD-sensitive structural changes. From nonlinear regression analysis of the titration data using the equation for a weighted one-site hyperbola, the following values were obtained for the concentration of metal ion effectuating 50% of the maximal change in ellipticity: $C_{50Ca-CD}$ for PC[1−47] = 0.86 mM; $C_{50Ca-CD}$ for PC[1−47-di-tBu] = 0.81 mM; $C_{50Mg-CD}$ for PC[1−47] = 0.87 mM; $C_{50Mg-CD}$ for PC[1−47-di-tBu] = 0.58 mM.

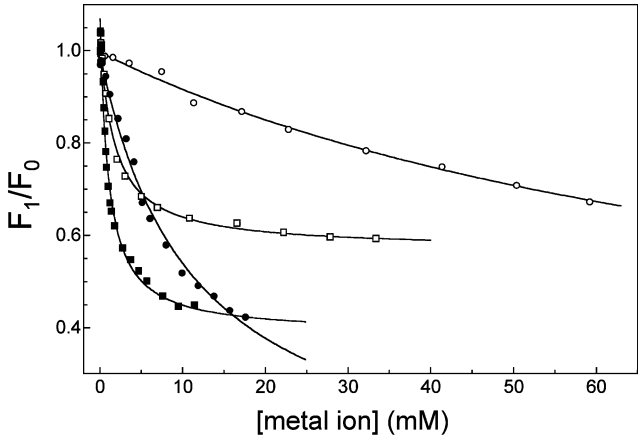

FIGURE 2: Metal ion-induced quenching of the intrinsic tryptophan fluorescence of PC[1−47] and PC[1−47-di-tBu]. Peptides were titrated with incremental additions of $CaCl_2$ or $MgCl_2$. Excitation and emission wavelengths were 280 and 340 nm, respectively. Fluorescence quenching is represented by the ratio, F_1/F_0, where F_1 is the fluorescence intensity at a given metal ion concentration and F_0 is the fluorescence in the absence of any added metal ion. Key: (■) PC[1−47] + Ca^{2+}; (●) PC[1−47-di-tBu] + Ca^{2}; (□) PC[1−47] + Mg^{2+}; (○) PC[1−47-di-tBu] + Mg^{2+}.

Further characterization of metal ion-induced conformational alterations in the 47-mers was achieved by monitoring changes in the intrinsic fluorescence of W41 as a function of Ca^{2+} and Mg^{2+} concentrations. After the data were fitted to a weighted one-site hyperbola, distinct differences were evident between the wild-type and alkylated peptides in both the Ca^{2+} and Mg^{2+} titration experiments (Figure 2). In the Ca^{2+} experiment, the $C_{50Ca-FL}$ values for PC[1−47] and PC-[1−47-di-tBu] were 1.02 and 11.1 mM, respectively. The maximum intrinsic fluorescence quenching (ΔF_{max}) was

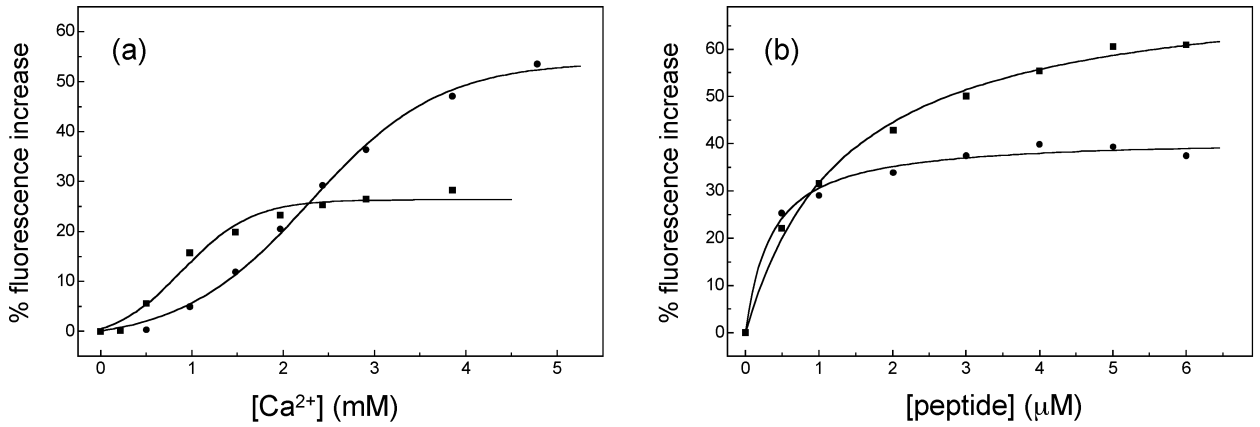

FIGURE 3: Interaction of PC[1−47] and PC[1−47-di-tBu] with PL vesicles as probed by fluorescence energy transfer. Acidic PL vesicles containing 10% dansyl-PE were titrated with either $CaCl_2$ (at constant peptide concentration) or the peptides (at constant Ca^{2+} concentration). Samples were excited at 280 nm, and the emission fluorescence intensity was monitored at 520 nm. The percent increase in fluorescence intensity was calculated as $(I - I_0)/I_0 \times 100$, where I is the intensity at a given Ca^{2+} or peptide concentration and I_0 is fluorescence associated with the PL vesicles prior to initiation of the titration. The vesicle concentration for all experiments was 16 μg/mL. (a) Increase in fluorescence energy transfer as a function of increasing Ca^{2+} concentration. Peptide concentration was maintained at 3 μM. Key: (■) PC[1−47]; (●) PC[1−47-di-tBu]. (b) Increase in fluorescence energy transfer as a function of increasing peptide concentration. Ca^{2+} concentration was maintained at 2 mM. Key: (■) PC[1−47]; (●) PC[1−47-di-tBu].

determined to be 68% for wild-type peptide and 95% for the alkylated species. For PC[1−47], the data from the Mg^{2+} titration corresponded to a $C_{50Mg-FL}$ of 1.80 mM and a ΔF_{max} of 46%. For PC[1−47-di-tBu], the $C_{50Mg-FL}$ and ΔF_{max} were 91.3 mM and 81%, respectively.

Contribution of the Disulfide Loop to PL Vesicle Binding. Interactions of the wild-type and alkylated 47-mers with mixed, acidic PL vesicles were studied by fluorescence energy transfer. In these experiments, vesicle-integrated dansyl-PE functioned as the reporter of peptide proximity to the bilayer. The effect of increasing Ca^{2+} on the ability of the peptides to bind PL vesicles is shown in Figure 3a. The $C_{50Ca-FET}$ values, determined from the Ca^{2+} midpoint of the limiting slopes at the beginning and end of the titration, were 0.90 mM for PC[1−47] and 2.30 mM for PC[1−47-di-tBu]. Despite the apparent higher affinity of the wild-type peptide for Ca^{2+}, the alkylated variant was more effective at facilitating energy transfer under conditions of saturating Ca^{2+} (maximal ratio of dansyl fluorescence intensity was extrapolated to 26% and 54% and for PC[1−47] and PC[1−47-di-tBu], respectively). In a related experiment, the increase in energy transfer as a function of peptide concentration was measured at constant Ca^{2+} concentration (2 mM). The $C_{50pep-FET}$ of the wild-type species was nearly 4-fold higher than that of the alkylated peptide (1.35 versus 0.35 μM) and was characterized by a higher ratio of dansyl fluorescence intensity (74% versus 41%) at infinite peptide concentration.

Relationship of the Intact Disulfide Loop to Ca^{2+}-Mediated sEPCR Binding. The relative ability of PC[1−47] and PC[1−47-di-tBu] to interact with sEPCR was evaluated by SPR. In our initial immobilization strategy, we attempted to link sEPCR to the chip surface using standard amine coupling. However, this resulted in an immobilized version of sEPCR that was insensitive to both PC[1−47] and PC[1−47-di-tBu]. APC also failed to exhibit a demonstrable response with amine-coupled sEPCR. This problem was circumvented by attaching sEPCR to the sensor chip using thiol coupling, as outlined by the manufacturer. The Ca^{2+}-dependent binding of the peptides to sEPCR was evaluated by injecting various concentrations of the peptides over the sEPCR-coupled surface in the presence of running buffer containing 5 mM Ca^{2+}. As shown in Figure 4a for PC[1−47], the magnitude of response was dependent upon the concentration of injected peptide. No response was observed with Ca^{2+}-free running buffer (data not shown). Saturation binding isotherms for wild-type and alkylated peptides, determined from the RU values at steady state, are depicted in Figure 4b. Fitting of the data to a single-site hyperbola yielded C_{50SPR} values of 37.1 and 2.6 μM for PC[1−47] and PC[1−47-di-tBu], respectively. This nearly 15-fold increase in sEPCR affinity of the alkylated analogue compared to the wild-type 47-mer was offset by a 3-fold reduction in maximal response of the alkylated versus wild-type species at saturation (PC[1−47] = 273 RU; B_{max}(PC[1−47-di-tBu]) = 92 RU).

DISCUSSION

Using synthetic peptide analogues of the GD-PC, we have investigated the contribution of the conserved hexapeptide disulfide loop to Ca^{2+}-mediated conformation, interactions with acidic PL vesicles, and sEPCR binding. To minimize the amount of derivatized Gla required for the Fmoc solid-phase synthesis of the GD-PC peptides, a single synthesis was conducted, employing N^{α}-Fmoc-(*S*-tBu)-L-Cys at positions 17 and 22 in the 47-mer sequence. Since the tBu-protected thiol group is impervious to TFA, standard TFA deprotection of the peptide-resin furnished product with the hexapeptide loop disrupted through *tert*-butylation. Half of this material was treated with $Hg(OAc)_2$, followed by air oxidation under high dilution to afford peptide with an intact, nativelike disulfide loop. Compared with the internal Cys−Cys linkage, *tert*-buylation of the Cys side chains can be classified as a radical "mutation". However, the considerable steric bulk associated with the *tert*-butyl groups hinders through-space proximity of C17 and C22, presumably minimizing the population of peptide conformers that mimic the native hexapeptide loop structure. Hence, the presence of the *tert*-butyl groups not only blocks disulfide loop formation but precludes adoption and/or minimizes the lifetimes of "disulfide loop-like" conformations.

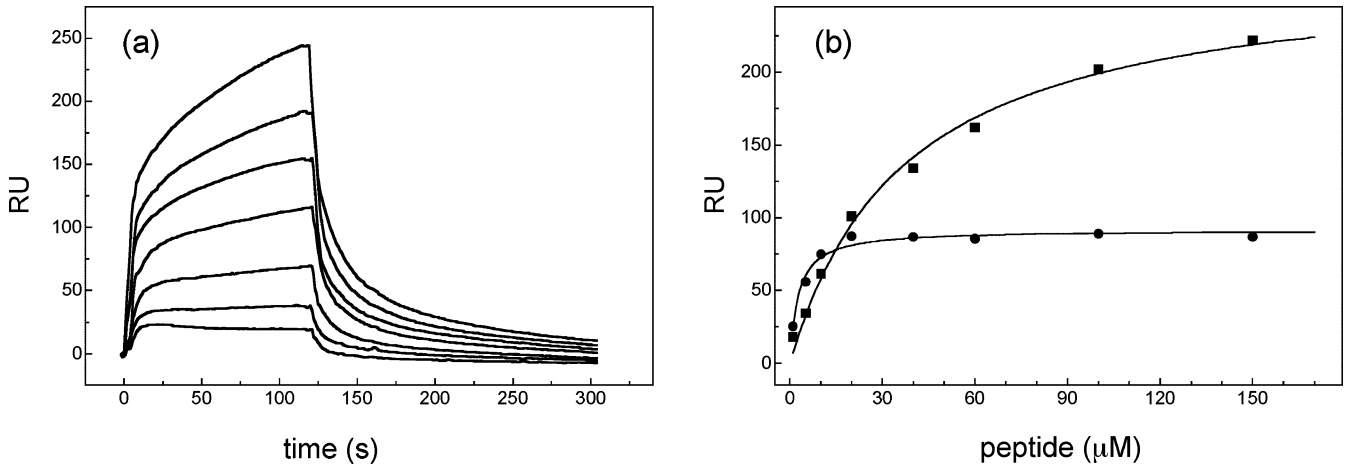

FIGURE 4: SPR analysis of the Ca^{2+}-dependent binding of PC[1−47] and PC[1−47-di-tBu] to sEPCR. (a) Representative overlay of sensorgrams obtained from the injection of various concentrations of PC[1−47] over immobilized sEPCR. Peptide was injected at a flow rate of 5 μL/min in running buffer that contained 5 mM $CaCl_2$. The concentration of peptide introduced was 1, 5, 10, 20, 40, 60, and 100 μM (bottom to top). A wash with running buffer was implemented at 120 s. (b) Dependence of the SPR response on the concentration of the PC Gla domain peptides. The RU values at each peptide concentration correspond to the averaged response of the final 5 s of the injection phase. Key: (■) PC[1−47]; (●) PC[1−47-di-tBu].

As monitored by CD, elimination of the disulfide bond in the GD-PC 47-mer results in a species that presents minimal secondary structure at saturating Ca^{2+} concentrations (Figure 1a). In terms of helicity, marginal content (2%) is associated with Ca^{2+}-loaded PC[1−47-di-tBu], while the unaltered peptide manifests ca. 10% helicity. This potential link between the hexapeptide loop and maintenance of helical elements is consistent with the results of a previous crystallographic study on the Gla domain of Ca^{2+}-bovine prothrombin fragment 1 (*25*) and with the NMR-derived structure of the Ca^{2+}-loaded GD-FIX (*26*). In these studies, it is seen that the hexapeptide loop (C18−C23) not only approximates a helical turn but bridges an immediately preceding single helical turn (residues 14−17) and two C-terminally adjacent turns of helix (residues 25−31). Similar helical elements are observed in the crystal structure of the GD-PC bound to sEPCR (*18*). Therefore, it is not unlikely that disruption of the disulfide linkage would diminish secondary structure, as observed in Ca^{2+}-complexed PC[1−47-di-tBu]. Both the alkylated and wild-type PC peptides exhibited negligible helical content in the absence of metal ion. This is somewhat unexpected since the C-terminal HS motif, an independent domain, is apparently retained in metal-free factor IX peptides (*27*, *28*) as well as apoprothrombin fragment 1 (*29*). In contrast to CD studies with factor IX (*28*), the population of apo-PC conformers bearing an ordered HS may simply be too low to be detected among the averaged global ensemble of structures.

Despite evoking a reduction in metal ion-induced secondary structure, Cys alkylation is without effect on the Ca^{2+}/Mg^{2+} binding sites involved in the CD-monitored conformational change. This is demonstrated by the nearly equivalent C_{50} values attending the Ca^{2+} and Mg^{2+} titrations of both PC[1−47] and PC[1−47-di-tBu] (Figure 1b). However, a different picture emerges with respect to the Ca^{2+}/Mg^{2+} sites involved in the quenching of W41 fluorescence (Figure 2). Not only is the extrapolated maximum for Ca^{2+}- and Mg^{2+}-induced quenching greater for the alkylated peptide, but the $C_{50Ca-FL}$ and $C_{50Mg-FL}$ values associated with the conformational transition of PC[1−47-di-tBu] are considerably higher (11-fold for Ca^{2+} and 50-fold for Mg^{2+}) than those determined from the wild-type titrations. These data are consonant with the previously mentioned structural work on prothrombin fragment 1 and the factor IX Gla domain. These studies revealed a substantial reorientation of W42 (prothrombin/factor IX numbering) between the apo and Ca^{2+}-complexed structures (*25*−*27*, *29*). More importantly, this shift can be ascribed to intimate contacts between the disulfide bond of the hexapeptide loop and the π-electrons of the indole ring of W42 that are noted in the presence, but not absence, of Ca^{2+}. Because the metal ion affinities obtained from the CD and fluorescence titrations of the PC peptides are differentially responsive to the presence of an intact C17−C22 disulfide bond, it can be reasonably concluded that the Gla−metal ion interactions responsible for helix induction are distinct from those that mediate the conformational transition reported by Trp fluorescence. In other words, the metal ion affinities for those binding sites that influence secondary structure are not perturbed by the disruption of the disulfide loop. However, metal ion binding at those sites that mediate tertiary folding is substantially diminished in the absence of the disulfide loop. On the basis of a modeled version of the GD-PC (*30*), candidate residues involved in this latter group of sites include Gla19 and Gla20, which are bridged by Ca-6, and Gla14 and Gla20, which coordinate Ca-7. Without the rigidity imposed by the C−C linkage, distorted or exceedingly flexible carboxylate geometries may prevail at these sites, leading to compromised metal ion binding.

In terms of Ca^{2+}-mediated interaction with PL vesicles, the alkylated PC peptide manifests a modest reduction in Ca^{2+} affinity (2.5-fold) compared to its wild-type counterpart (Figure 3a). Previous studies with recombinant PC mutants have identified Gla residues 7, 16, 20, and 26 as critical participants in the Ca^{2+}-induced conformation that is necessary for PL vesicle binding. The present data suggest that the optimal orientation of these residues is not significantly perturbed when the hexapeptide loop is disrupted. At saturating Ca^{2+}, PC[1−47-di-tBu] is twice as efficient as PC[1−47] at promoting energy transfer from W41 to dansyl-PE in the bilayer. The alkylated peptide may simply bind with higher stoichiometry, possibly facilitated by the hydrophobic *tert*-butyl groups, which could embed to some degree

in vesicles. Alternatively, the PL-bound alkylated peptide might assume a conformation in which W41 is more proximal to the dansyl group than in the PC[1−47]/PL vesicle complex.

In a related experiment, PL vesicle binding was probed as a function of increasing peptide concentration. The Ca^{2+} concentration was maintained at 2 mM, a level that provided for similar fluorescence increases for both the alkylated and wild-type peptide (Figure 3a). The results indicate that the elimination of the disulfide bond does not adversely affect the ability of the GD-PC to interact with the membrane (Figure 3b). In fact, PC[1−47-di-tBu] manifested a 4-fold enhanced affinity for acidic PL vesicles compared to the wild-type peptide. Increased conformational flexibility of the alkylated species may account for this outcome, although the hydrophobic nature of the *tert*-butyl groups may also augment peptide interaction with PL vesicles. In another reversal from the Ca^{2+} titration, PC[1−47-di-tBu] is less efficient than PC[1−47] at promoting energy transfer at saturation. At 2 mM Ca^{2+}, fewer metal ion binding sites are occupied in the alkylated species (Figures 2 and 3a), resulting in a conformation that may interact differently with PL vesicles.

As investigated by SPR analyses, disruption of the hexapeptide loop actually augments peptide binding to immobilized sEPCR by over an order of magnitude. It bears noting that the absolute K_d values derived from these SPR experiments (37.1 μM for PC[1−47]; 2.6 μM for PC[1−47-di-tBu]) are considerably higher than the recently reported value for the SPR-monitored binding of full-length PC to sEPCR (K_d = 147 nM) (*31*). A possible explanation for this discrepancy may lie in the difference in sEPCR immobilization strategies between the two studies, i.e., direct thiol-mediated coupling of sEPCR to the sensor chip (this study) versus noncovalent immobilization of sEPCR via an anti-EPCR antibody coupled directly to the chip (*31*). In the present study, EPCR immobilization proceeded through thiol−disulfide exchange of an unpaired cysteine (C97) at the disulfide-derivatized chip surface. It is conceivable that this particular immobilization strategy somehow compromises the interaction of EPCR and the GD peptides. However, crystallographic data reveal that C97 is present on the β-sheet scaffold of EPCR, far removed from the GD binding site located at the portal of a deep groove that is formed by two antiparallel α-helices (*18*). In the same study, a single PL molecule, tightly bound within the groove, cocrystallized with the EPCR/PC and was shown to be necessary for PC-GD binding. Because C97 is proximal to the tail of the PL, some perturbation of PL binding (and, by extension, of PC-GD binding) may occur upon C97-mediated surface immobilization. Alternatively, despite overarching evidence that points to the GD as the sole mediator of PC-EPCR contacts (*13*, *31*), the isolated domain may be too flexible and/or otherwise incapable of adopting the optimal conformation for tight docking with EPCR [even though the Ca^{2+}- and PL-binding properties of full-length PC are fully reproduced by PC[1−47] (*8*)]. This notion is supported by competition binding studies in which the K_i for inhibition of ^{125}I-APC binding to cell surface EPCR was determined to be 100 nM for unlabeled PC but 2 μM for a GD peptide (*13*). Hence, the micromolar range K_d values of PC[1−47] and PC[1−47-di-tBu] obtained in this study may reflect the inability of isolated PC-GD to completely mimic the Ca^{2+}-induced conformation adopted in the context of full-length PC. It is not unreasonable to conclude that the results of the SPR studies reported herein reflect EPCR affinities that are valid in a relative, if not absolute, sense.

The increased affinity of PC[1−47-di-tBu] is accompanied by a reduction in maximal response. The latter observation is most simply explained in terms of reduced receptor occupancy by the alkylated peptide. Myriad reasons for this outcome can be forwarded, but we also note that amine coupling of sEPCR to the sensor chip resulted in an immobilized species that was incapable of PC peptide binding. This problem was circumvented through thiol coupling of sEPCR to the chip surface, although some degree of heterogeneity in sEPCR orientation may have arisen from this immobilization chemistry, yielding receptor forms that are insensitive or inaccessible to the alkylated species. High sEPCR density on the chip surface may also be a factor in the reduced maximal response, preferentially hindering the access of PC[1−47-di-tBu] to the receptor binding site.

A complex comprised of sEPCR, the GD-PC, and a single phospholipid molecule has revealed that the disulfide loop is not involved in any direct contacts with either EPCR or lipid (*18*). In fact, surprisingly few intermolecular contacts appear to be mediating PC binding to EPCR. These include ω-loop residues F4 and L8, which interact with a hydrophobic patch formed by L82, Y154, and T157 of EPCR. Other PC residues within hydrogen-bonding distance of EPCR side chains include Gla7, Gla25, and Gla29. All of the PC residues implicated in EPCR contacts are sequentially and spatially removed from the disulfide loop. This does not rule out thermodynamic linkage between the disulfide bond and PC residues that contact the EPCR. The loop may also contribute to the dynamic properties of the GD peptide backbone, impacting EPCR recognition and docking. However, our SPR results indicate that the absence of the disulfide loop motif does not impart any deleterious effects on PC affinity for the EPCR. In fact, disruption of the disulfide bond leads to an increase in peptide affinity for the receptor. The molecular basis for this finding may relate to the reduction in secondary structure (i.e., greater flexibility) of PC[1−47-di-tBu] compared with PC[1−47]. Greater conformational mobility of a ligand frequently results in enhanced affinity for its cognate receptor by allowing multiple functional groups to orient freely. This unconstrained motion can allow the ligand to be optimally accommodated with respect to receptor binding site geometry (*32*, *33*). We have previously noted that amino acid substitutions which increase the conformational flexibility of the Gla-rich conantokin peptides can lead to increased potency with respect to the NMDA receptor, their physiological target (*34*). Similar motional considerations may be mediating the enhanced affinity of the alkylated PC peptide for sEPCR.

In conclusion, the present study demonstrates that the absence of a disulfide linkage between C17−C22 of the GD-PC imparts significant changes in the Ca^{2+}-induced structure of the peptide. However, disruption of this motif, and the accompanying diminution of secondary structure, is without substantial effect on PL vesicle binding and actually augments sEPCR binding. As the pivotal role of PC in mitigating inflammation and apoptosis becomes increasingly evident, the continued elaboration of structure−function relationships

in PC, with emphasis on EPCR recognition, will be of importance in the development of effective agents for the treatment of acute inflammatory responses.

ACKNOWLEDGMENT

We thank Professor Charles T. Esmon for providing the HPC4-tagged sEPCR.

REFERENCES

1. Esmon, C. T. (1993) Molecular events that control the protein C anticoagulant pathway, *Thromb. Haemostasis 70*, 29−35.
2. Sakata, Y., Loskutoff, D. J., Gladson, C. L., Hekman, C. M., and Griffin, J. H. (1986) Mechanism of protein C-dependent clot lysis: role of plasminogen activator inhibitor, *Blood 68*, 1218−1223.
3. Bajzar, L., Nesheim, M. E., and Tracy, P. B. (1996) The profibrinolytic effect of activated protein C in clots formed from plasma is TAFI-dependent, *Blood 88*, 2093−2100.
4. Griffin, J. H., Zlokovic, B. V., and Fernandez, J. A. (2002) Activated protein C: potential therapy for severe sepsis, thrombosis and stroke, *Semin. Hematol. 39*, 197−205.
5. Joyce, D. E., Gelbert, L., Ciaccia, A., DeHoff, B., and Grinnell, B. W. (2001) Gene expression profile of antithrombotic protein C defines new mechanisms modulating inflammation and apoptosis, *J. Biol. Chem. 276*, 11199−11203.
6. Esmon, C. T., Xu, J., Gu, J. M., Qu, D., Laszik, Z., Ferrell, G., Stearns-Kurosawa, D. J., Kurosawa, S., Taylor, F. B., Jr., and Esmon, N. L. (1999) Endothelial protein C receptor, *Thromb. Haemostasis 82*, 251−258.
7. Esmon, N. L., DeBault, L. E., and Esmon, C. T. (1983) Proteolytic formation and properties of gamma-carboxyglutamic acid-domainless protein C, *J. Biol. Chem. 258*, 5548−5553.
8. Colpitts, T. L., and Castellino, F. J. (1994) Calcium and phospholipid binding properties of synthetic gamma-carboxyglutamic acid-containing peptides with sequence counterparts in human protein C, *Biochemistry 33*, 3501−3508.
9. Mann K. G., Nesheim, M. E., Church, W. R., Haley, P., and Krishnaswamy, S. (1990) Surface-dependent reactions of the vitamin K-dependent enzyme complexes, *Blood 76*, 1−16.
10. Christiansen, W. T., and Castellino, F. J. (1994) Properties of recombinant chimeric human protein C and activated protein C containing the gamma-carboxyglutamic acid and trailing helical stack domains of protein C replaced by those of human coagulation factor IX, *Biochemistry 33*, 5901−5911.
11. Geng, J. P., and Castellino, F. J. (1997) Properties of a recombinant chimeric protein in which the gamma-carboxyglutamic acid and helical stack domains of human anticoagulant protein C are replaced by those of human coagulation factor VII, *Thromb. Haemostasis 77*, 926−933.
12. Smirnov, M. D., Safa, O., Regan, L., Mather, T., Stearns-Kurosawa, D. J., Kurosawa, S., Rezaie, A. R., Esmon, N. L., and Esmon, C. T. (1998) A chimeric protein C containing the prothrombin Gla domain exhibits increased anticoagulant activity and altered phospholipid specificity, *J. Biol. Chem. 273*, 9031−9040.
13. Regan, L. M., Mollica, J. S., Rezaie, A. R., and Esmon, C. T. (1997) The interaction between the endothelial cell protein C receptor and protein C is dictated by the gamma-carboxyglutamic acid domain of protein C, *J. Biol. Chem. 272*, 26279−26284.
14. Zhang, L., Jhingan, A., and Castellino, F. J. (1992) Role of individual gamma-carboxyglutamic acid residues of activated human protein C in defining its in vitro anticoagulant activity, *Blood 80*, 942−952.
15. Zhang, L., and Castellino, F. J. (1993) The contributions of individual gamma-carboxyglutamic acid residues in the calcium-dependent binding of recombinant human protein C to acidic phospholipids vesicles, *J. Biol. Chem. 268*, 12040−12045.
16. Zhang, L., and Castellino, F. J. (1991) Role of the hexapeptide disulfide loop present in the γ-carboxyglutamic acid domain of human protein C in its activation properties and in the in vitro anticoagulant activity of activated protein C, *Biochemistry 30*, 6696−6704.
17. Fukudome, K., and Esmon, C. T. (1994) Identification, cloning, and regulation of a novel endothelial cell protein C/activated protein C receptor, *J. Biol. Chem. 269*, 26486-26491.
18. Oganesyan, V., Oganesyan, N., Terzyan, S., Qu, D., Dauter, Z., Esmon, N. L., and Esmon, C. T. (2002) The crystal structure of the endothelial protein C receptor and a bound phospholipids, *J. Biol. Chem. 277*, 24851−24854.
19. Colpitts, T. L., and Castellino, F. J. (1993) Binding of calcium to synthetic peptides containing gamma-carboxyglutamic acid, *Int. J. Pept. Protein Res. 41*, 567−575.
20. Prorok, M., Warder, S. E., Blandl, T., and Castellino, F. J. (1996) Calcium binding properties of synthetic γ-carboxyglutamic acid-containing marine cone snail "sleeper" peptides, conantokin-G and conantokin-T, *Biochemistry 35*, 16528−16534.
21. Chen, Y.-H., Yang, J. T., and Martinez, H. M. (1972) Determination of the secondary structures of proteins by circular dichroism and optical rotatory dispersion, *Biochemistry 11*, 4120−4131.
22. Jacobs, M., Freedman, S. J., Furie, B. C., and Furie, B. (1994) Membrane binding properties of the factor IX gamma-carboxyglutamic acid-rich domain prepared by chemical synthesis, *J. Biol. Chem. 269*, 25494−25501.
23. Beals, J. M., and Castellino, F. J. (1986) The interaction of bovine factor IX, its activation intermediate, factor IX alpha, and its activation products, factor IXa alpha and factor IXa beta, with acidic phospholipid vesicles of various compositions, *Biochem. J. 236*, 861−869.
24. Fukudome, K., Kurowawa, S., Stearns-Kurowawa, D. J., He, X., Rezaie, A. R., and Esmon, C. T. (1996) The endothelial cell protein C receptor, *J. Biol. Chem. 271*, 17491−17498.
25. Soriano-Garcia, M., Padmanabhan, K., de Vos, A. M., and Tulinsky, A. (1992) The Ca^{2+} ion and membrane binding structure of the gla domain of Ca-prothrombin fragment 1, *Biochemistry 31*, 2544−2566.
26. Freedman, S. J., Furie, B. C., Furie, B., and Baleja, J. D. (1995) Structure of the calcium ion-bound γ-carboxyglutamic acid-rich domain of factor IX, *Biochemistry 34*, 12126−12137.
27. Freedman, S. J., Furie, B. C., Furie, B., and Baleja, J. D. (1995) Structure of the metal-free γ-carboxyglutamic acid-rich membrane binding region of factor IX by two-dimensional NMR spectroscopy, *J. Biol. Chem. 270*, 7980−7987.
28. Vysotchin, A., Medved, L. V., and Ingham, K. C. (1993) Domain structure and domain-domain interactions in human coagulation factor IX, *J. Biol. Chem. 268*, 24339−24345.
29. Seshadri, T. P., Tulinsky, A., Skrzypczak-Jankun, E., and Park, C. H. (1991) Structure of bovine prothrombin fragment 1 refined at 2.25 Å resolution, *J. Mol. Biol. 220*, 481−494.
30. Christiansen, W. T., Tulinsky, A., and Castellino, F. J. (1994) Functions of individual g-carboxyglutamic acid (gla) residues of human protein C. Determination of functionally nonessential Gla residues and correlations with their mode of binding to calcium, *Biochemistry 33*, 14993−15000.
31. Preston, R. J. S., Villegas-mendez, A., Sun, Y.-H., Hermida, J., Simioni, P., Philippou, H., Dahlbäck, B., and Lane, D. A. (2005) Selective modulation of protein C affinity for EPCR and phospholipids by Gla domain mutation, *FEBS J. 272*, 97−108.
32. Benveniste, M., and Mayer, M. L. (1991) Stucture−activity analysis of binding kinetics for NMDA receptor competitive antagonists: the influence of conformational restriction, *Br. J. Pharmacol. 104*, 207−221.
33. Perola, E., and Charifson, P. S. (2004) Conformational analysis of drug-like molecules bound to proteins: an extensive study of ligand reorganization upon binding, *J. Med. Chem. 47*, 2499−2510.
34. Warder, S. E., Blandl, T., Klein, R. C., Castellino, F. J., and Prorok, M. (2001) Amino acid determinants for NMDA receptor inhibition by conantokin-T, *J. Neurochem. 77*, 812−822.

BI050974+